Int. J. Electrochem. Sci., 15**(2020)** 7448 – 7458, doi: 10.20964/2020.08.77

International Journal of
ELECTROCHEMICAL
SCIENCE
www.electrochemsci.org

Short Communication

Electrodeposition and Characterization of Mesoporous Nanostructured Cobalt Films

Ahmed A. Al Owais[1], *Ibrahim S. El-Hallag*[2,*], *Elsayed El-Mossalamy*[3]

[1] Chemistry Department, College of Science, King Saud University, Riyhad, Saudi Arabia
[2] Chemistry Department, Faculty of Science, Tanta University, Tanta, Egypt.
[3] Chemistry Department, Faculty of Science, Benha University, Benha, Egypt.
[*]E-mail: i.elhallag@yahoo.com

Received: 20 February 2020/ *Accepted:* 14 May 2020 / *Published:* 10 July 2020

In this article we demonstrate a simple and versatile technique for the fabrication of mesoporous films of cobalt using Brij-76 surfactant which is used as the template for exhibiting the three-dimensional highly ordered deposited films. It was found that the films containing arrays are closed and packed in a uniform size and spherical holes. Here the mesoporous cobalt films were prepared electrochemically. Also, different potential techniques were used for investigation and description the properties of the plated mesopores of Co films.

Keywords: Nanostructured, mesoporous, Electrodeposition, Brij76, Cyclic voltammetry.

1. INTRODUCTION

Mesoporous materials exhibited very interesting properties such as electrical conductance, optical-activity, magnetic and chemical feature which provide good characteristics more than that in their bulk dimensions [1]. It was observed that the mesoporous materials are used in radiographic techniques, accumulation of a drug molecule in the target organ, and other important applications in catalysis and biological study [2].

The developing of the electrochemical capacitors (ECs) is due to their longer life cycle and their energy density that is greater than that of conventional electrical double-layer capacitors [3].

Trasatti [4]; Sarangapani et al. [5]; Andrew [6]; Zhao *et. al.* [7] had reported that, the applications of electrochemical capacitors (ECs) display very important roles in the sources of power such as supplementary sources of power for electronic smartphones,…. *etc*.

The storing of energy at the interface between an electrolyte/electrode via electrochemical capacitors was utilised by a charged double layer and interfacial redox processes. It was established

that the size of the pore at the range of 2 nm to 50 nm (mesopores) is believed to be highly appropriate for the electrochemical ultra-capacitors, and the arranged mesopore makes ionic motion easier compared with conventional mesopore material in which the pores are randomly connected [8].

From the phase graph cited in publications the percentage composition of the hexagonal form of the Brij76/Co/p-xylene structure was established [9, 10]. The surfactant molecules were used as templates in case of formation of nano pore materials and was found to be a very effective area of research [11, 12]. The surfactant molecules congregate into elongate cylindrical micelles and these micelles which then arrange into a hexagonal array like (Figure 1) in which the distance between them - the micelles is corresponding to their bore approximately 2 nm [13]. In case of using brij76 as a template in the deposition of metal films via application of electrical energy, the electrolyte and metal salt are decomposed into the aqueous part of the composition and metal deposition takes place round the molecules of surfactant micelles. Washing process is used to eliminate surface active molecules, when electroplating is complete to exhibits ordered hexagonal of matrices of identical pores of metal film. The depth of the deposited film is increased by increasing the quantity of charging passed.

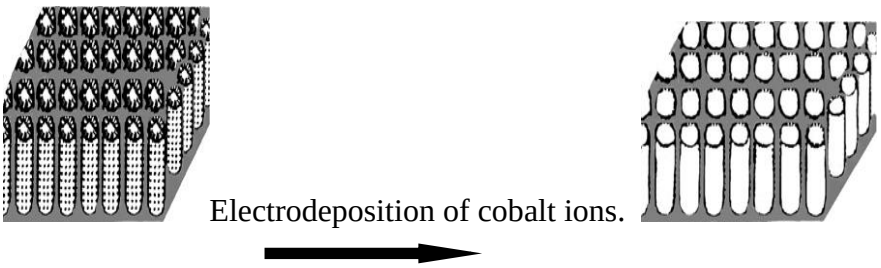

Figure 1. Illustrate the progress method of the electrodeposited mesoporeH1-e Co films and elimination of the template.

In this article the formation of the mesopore nanostructured cobalt films (H1-eCo) was performed using aqueous media of the hexagonal liquid crystal phase of Brij 76.

Scanning electron microscopy (SEM), transmission electron microscopy (TEM) and X-ray diffraction techniques were used for inspection of the arrangement of the H_1-eCo layers. Cyclic sweep voltammetry (CV) and chronoamperometry were used for clarification the properties of the electroplated Co films.

2. EXPERIMENTAL

2.1. Chemicals and Materials

Polyoxyethylene (10) stearyl ether (Brij-76) surfactants has structural formula $C_{18}H_{37}(OCH_2CH_2)_{10}OH$, and it is purchased from Aldrich. Using reagent category (18 MΩ cm) all

solutions & liquid crystalline template (LCT) were prepared. The cleaning of glassware was performed by soaking it in 5% Decon 90 (Aldrich solution for few days followed by rinsing with double distilled water and drying it in an oven at 50ºC. P-xylene (99%), acetate salts of cobalt (CoAc2.4H2O 99.5 %), potassium (KAc 99%) and boric acid (H_3BO_3) were acquired from Aldrich. Ternary system made up of Brij76 non-ionic surfactant ($C_{20}H_{42}O_2$), aqueous solution of $CoAc_2.4H_2O$, H_3BO_3 and p-xylene have been used in this work. The H_1 phase of ternary mixture containing 53.13 wt % aqueous Co salts and boric acid, 44.6% weight of Brij 76 and 2.23% weight of p-xylene which is chemically fixed for greater than four weeks at room temperature. At the end of deposition, the electrodes were washed with extra quantities of deionized water to get rid of the surfactant. The cleaning of the gold electrode was performed by sonication in propanol (BDH) for 1 h accompanied by cleaning with deionized water [14].

2.2. Electrochemical Analysis Measurements

Using an EG & G 283 Potentiostat and a normal three electrode cell were used in the electrochemical experiments. The electrodes used in the measurements are 0.5mm radius gold disk electrode, 1 cm^2 sheet electrode for the structural description of the performed material films. Counter & reference electrodes used hither are platinum gauze of area one cm^2 and saturated calomel electrode (SCE) respectively. Cleaning paper (class 1200) accompanied by alumina (Buehler) of two grades: 1.0 and 0.3 μm was used for cleaning the gold disc electrode. The captured cyclic voltammograms were recorded at various scan rates in the range of 5mV.s^{-1} to 1000 mV.s^{-1}. An analytical SEM (JOEL 6400) was used to investigate the morphology and depth of the electrodeposited cobalt films. Analysis of SEM samples was performed by depositing Co electrochemically from the framework mixture on to evaporated gold electrodes (area 1 cm^2). In an ultrasonic bath of 2-propanol, these gold sheet electrodes were cleaned for 10 min instantaneously previous to use. To show primary validation for the fabrication of a nanostructured film XRD with Cu Kα radiation was used. JEOL 2000FX transmission electron microscope working at an accelerating voltage of 200 KV was used to indicate the arrangement of the nanostructure.

3. RESULTS AND DISCUSSION

3.1. Constructal Investigation

Polarized-light optical microscopy (POM) and low-angle XRD have been used afore electrodeposition to complete the electrolyte phases structure. Figure 2 shows the typical POM images for Brij76 template Cobalt. The figure displays that, the spacing between the three axes on the same plane equal 120 º which confirming the creation of hexagonal structure [15].

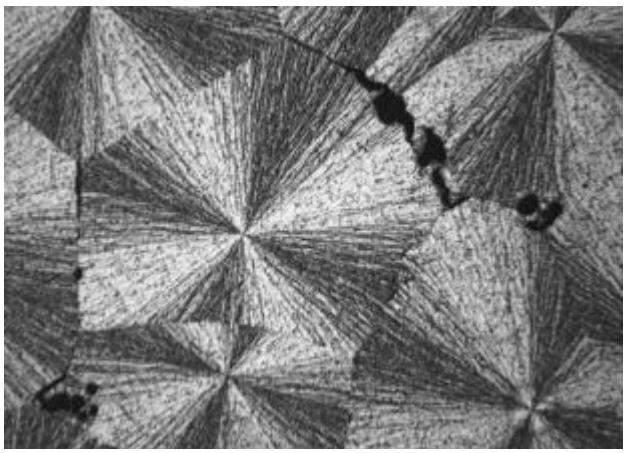

Figure 2. Image of polarized-light optical microscopy for Brij76 templated CoAc2.

3.2. SEM and TEM of cobalt/Brij76 films.

The final deposited film of the nanoarchitecture form is determined directly via the structure of the lyotropic phase used of deposition process [9,10,16]. The electrochemically deposited cobalt films at –0.92 V *vs*. SCE from template mixture have a metallic luster of silver appearance and held properly to the vaporized gold electrodes used for the deposition. Figure 3A displays SEM of an, electrodeposited hexagonal, H_1-eCo film indicating the cobalt film formed is featureless.

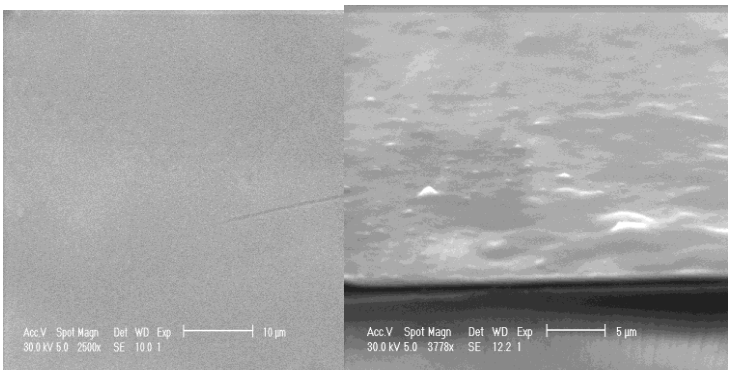

(A) **(B)**

Figure 3. SEM of electrodeposited H1-e Co layers in the presence of hexagonal liquid crystal pattern (A), Cross-section view of deposited Co film (B).

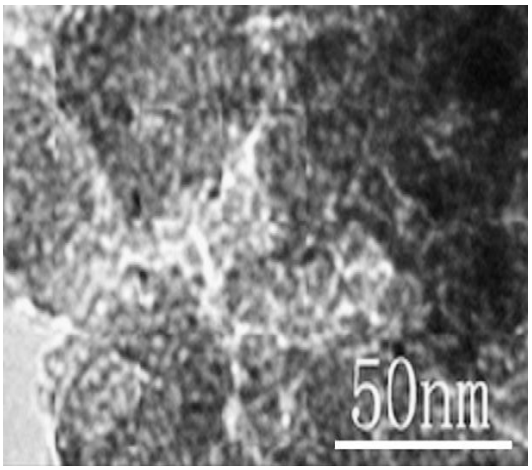

Figure 4. S TEM images of cobalt film at deposition potentials -0.92V.

Figure 3B exhibited that the cross-sectional view of the film is smooth, compact and uniformly. The film thickness is about 219 nm. There is no appearance for a structure on the nanosize noticeable on the scale of the SEM. So, TEM is essential to inspect the nano size of deposited cobalt films, as shown in Figure 4.

The above figure of TEM shows that the images have well-ordered arrays of hexagonal uniform mesoporous structure. It was noted that, after removing of the surfactant template, the deposition process exhibits bright zones accords to the pores of surfactant. The dark regions correspond to the electrodeposited cobalt metal.The captured images exhibit that the pores are arranged in a hexagonal shape. It is expected that when the cobalt is a casting of the lyotropic crystalline phase throughout the time it is a soft solid, these leads to minor departure from linearity and the appearance of some defects as mentioned formerly [17, 18].The center to center distance of the film has an 11.15 pore, with invariable pore diametre of around 9.2 nm and cobalt wall thickness of about 5.4 nm. It was indicated that, at different potentials for deposition, the nanostructures of the H_1-eCo almost remain unchanged as indicated in TEM results, which is agreed with the results recorded in literature[19 - 22]. On the basis of the distinguished portrayal of the pore size and wall thickness, a huge specific surface area within these pores would be expected. A high specific surface area inside these pores would be expected, according to the basis of the pore size and wall thickness. This is supported by X-ray investigation.

3.3. X-ray description of H_1-eCo films.

Figure 5 shows the low-angle XRD patterns of the Brij76 template Co electrolyte from CoAc2, which exhibits hexagonal symmetry with *d* spacing of 7. 53 nm and 4.83 nm for (100) and (110) reflections. As shown, a well-known higher intensity peak corresponding to a d-spacing of 7.53 nm are exhibited by the low angle XRD pattern for the electrodeposited cobalt. This is agreeable with the deposition of a cobalt film with a honey combed nanostructure resulting from the structure of the template mixture. However, the ordering of H_I-Co film is lower than the hexagonal liquid crystalline state of the template mixture as indicating by the nonappearance of higher diffraction levels and the

bore of H_I-Co at half maximum is much more exceeding the width of (100) a plane peak of the template mixture.

The pore -to- pore distance (r) for these hexagonal arrays provided by:

$$r = d_{110}/\cos 30 \quad (1)$$

is 8.54 nm. The following relationship is used for calculation of the width of the basic vector length (lattice parameter), a_h of the hexagonal phases [20]:

$$a_h = (2d/\sqrt{3}) \quad (2)$$

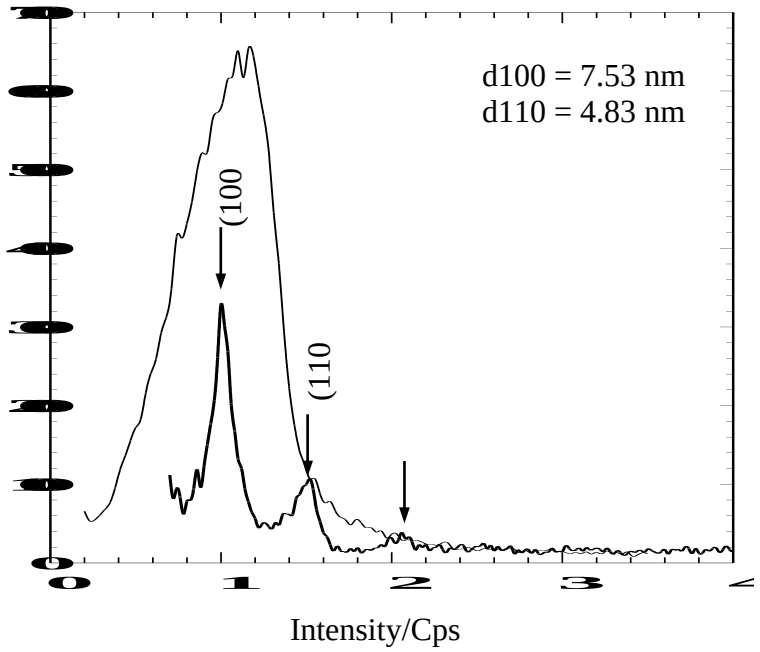

Figure 5. Low angle XRD (—) for the hexagonal lyotropic (H_I) liquid crystalline phase of pattern mixture, Low angle XRD (—) for a nanostructured H_I-eCo film deposited via haxagonal phase of the Brij® pattern admixture.

3.4. Cyclic voltammetry investigation

In this article, the electrochemical properties of electrodeposited cobalt film were characterised by cyclic voltammetry technique in 0.1 M NaOH at various scan rates. Figure 6 displays the characteristic CV curves of the cobalt film electrode at two different scan rates. It can be observed that the figure exhibits a pair of peaks corresponding to the redox reaction of cobalt film [23].

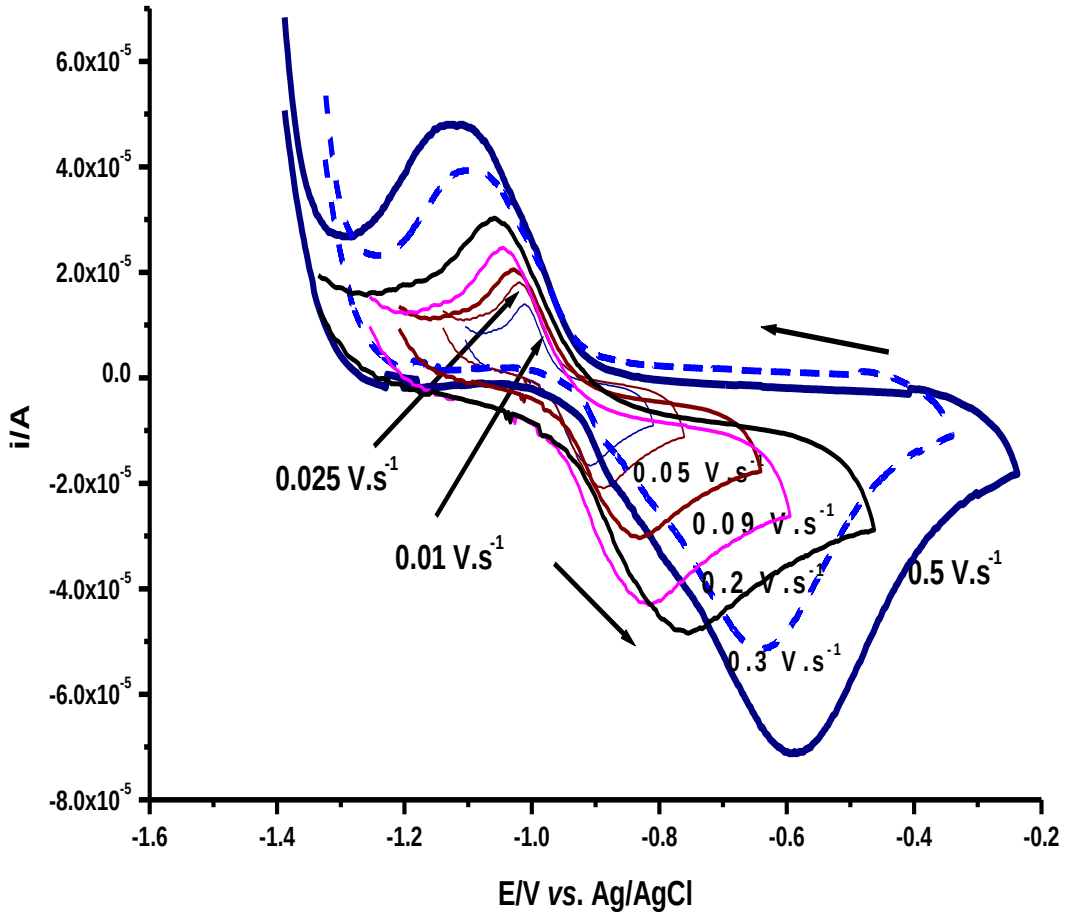

Figure 6. Cyclic voltammograms of electrodeposited cobalt film in 0.1M NaOH at various scan rates.

As indicated in the captured cyclic voltammograms the forward oxidative peak corresponding to the anodic peak (Epa) due to the oxidation of cobalt metal and the reversal reductive peak (Epc) corresponding to the cathodic peak (Epc) of cobalt ion. It was noted that, with increasing the scan rates the anodic peak potentials shift to less negative values, while the cathodic peak potentials shift to more negative values. Also, at all scan rates the peak separation (ΔEp) increase with increasing the scan rate confirming the moderate fast of electron transfer rate.

The peak current (i_p) can be expressed by the following equation:

$$i_p = 2.99x10^5\ n\ (\alpha n_a)^{1/2}\ AD^{1/2}Cv^{1/2} \qquad (3)$$

Where the symbol ip is referred to the peak current in amp, v is the scan rate in volt per second and the remaining terms have their usual definition. The plot of i_p vs. $v^{1/2}$ produces straight lines with

some slight deviation from the origin revealing that the diffusion character of the current with some adsorption contribution [16]. Also, it was observed that the values of (E_p – $E_{p/2}$) grow larger with increasing the scan rates, indicating increasingly the slow nature of the electrode process as the scan rates increase [16].

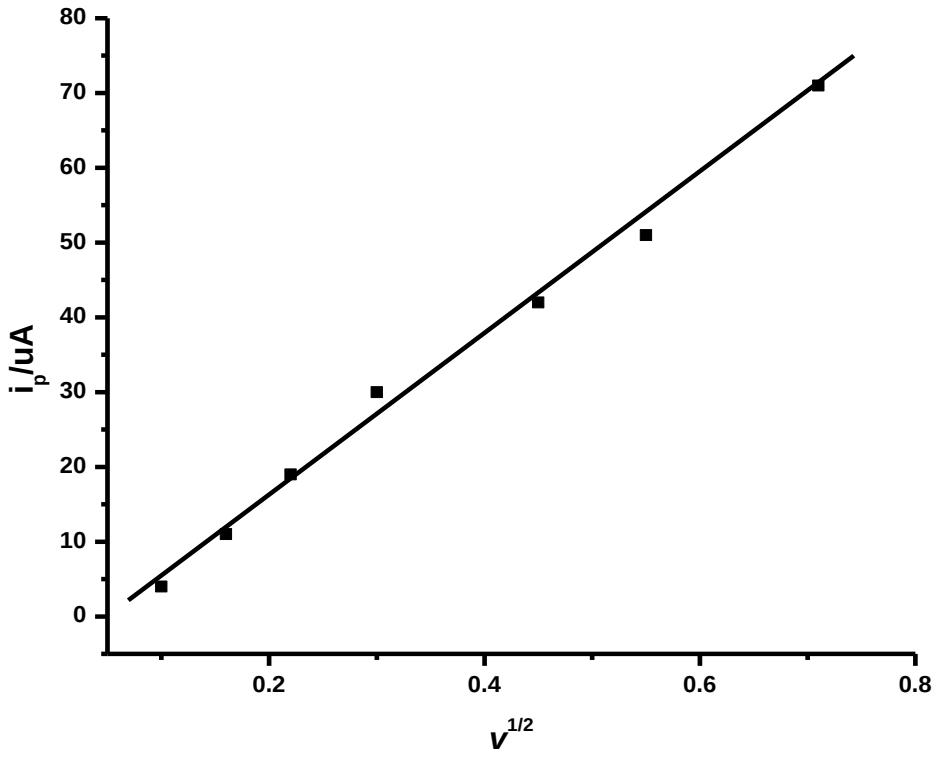

Figure 7. Dependence of i_p on $v^{1/2}$ $(V.s^{-1})^{1/2}$ of electrodeposited Co film from lyotropic liquid crystale Brij 76.

Figure 7 exhibits a linear dependence of i_p – $v^{1/2}$, and particularly the increase of the current in the peak with the square root of scan rate ($v^{1/2}$), evidence that the deposition of Co is a diffusion controlled process. It corresponds to diffusion controlled process with interference on the chemical stage preceding the reaction of discharge of Co^{2+} [24].

Table 1 summarizes the extracted peak parameters of the cobalt film via cyclic voltammograms at various scan rates. It was noted that the values of the forward peak current increase with increasing the scan rate and the magnitude of the peak separation become larger with increasing the values of scan rate.

Table 1. Show the obtained electrochemical parameters of deposited cobalt film.

Scan rate, ν, Vs^{-1}	ip/μA	ΔEp, V
0.010	4	0.070
0.025	11	0.090
0.050	19	0.120
0.090	30	0.185
0.200	42	0.290
0.300	51	0.450
0.500	71	0.630

The chronoamperometric response of Co^{2+} was recorded at a gold electrode in lyotropic liquid crystal template. Figure 8 shows the response of chronoamperograms (I - t) curves obtained by the electrodeposition of cobalt at gold electrode surface in Brij 76 template.

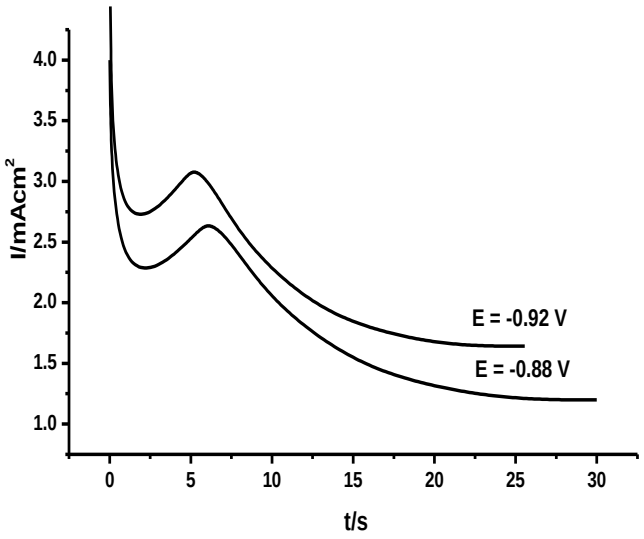

Figure 8. Current density obtained from chronoamperometry experiments of Cobalt(II)/Brij 76 at a gold electrode and at two different step potentials.

The decrease of current with time as a result of depletion of cobalt ion is smoother and is explained with the simultaneous growth mechanism of the nuclei formed (figure 8). It was found that in slightly acidic acetate electrolyte (pH = 5.2), cobalt present as free metal ion (Co^{2+}) [25, 26].

4. CONCLUSION

This article has provided an overview on fabrication and characterisation of electrodeposited mesoporous nanostructured cobalt Films using Lyotropic Liquid Crystal Phase. The electrodeposited films were investigated and characterised via SEM, TEM, XRD, cyclic voltammetry and chronoamperometry techniques. It was noted that, the formed films containing arrays which were closed and packed in a uniform size and spherical holes. The mesoporous cobalt films were prepared electrochemically. Here the formation of the mesopore nanostructured cobalt films (H1-eCo) was performed using aqueous media of the hexagonal liquid crystal phase of Brij 76.

ACKNOWLEDGEMENTS
This project was supported by King Saud University, Deanship of Scientific Research, College of Science Research Center.

References

1. V.L. Colvin , M.C. Schlamp and A.P. Alivisatos, *Nature*, 370 (1994) 354.
2. V. Kesavan, S.P. Sivanand, S. Chandrasekaran, Y. Kaltypin and A. Gedanken. *Angew. Chem. Int*., 38 (1999) 3521.
3. B.E. Conway, *J. Electrochem. Soc*., 138 (1991) 1539.
4. S. Trasatti and P. Kurzweil. *Platinum Met. Rev*., 38 (1994) 46.
5. S. Sarangapani, B.V. Tilak and C.P. Chen. *J. Electrochem. Soc*., 134 (1996) 3791.
6. A. Andrew, *J. Power Sources.*, 91(2000) 37.
7. D.D. Zhao, M.W. Xu, W.J. Zhou, J. Zhang and H.L. Li . *Electrochim.Acta*, 53 (2008) 2699.
8. S. Yoon, J. Lee, T. Hyeon and T.S. Oh . *J. Electrochem. Soc*., 147 (2000) 2507.
9. K.N. Raman, M.T. Anderson and C. Brinker. *J. Mater. Chem.*,8 (1996) 1682.
10. A. Paavola, J. Ylirusi and P. Rosenberg. *J. Controlled Release.,* 52 (1998) 169.
11. J. Liu, Y. Shin, Z. Nie, J. H. Chang, L.Q. Wang, G.E. Fryxell, W.D. Samuels and G.J. Exarhos. *J. Phys. Chem. A.*, 104 (2000) 8328.
12. M.E. Raimondi and J.M. Seddon. *Liq. Cryst*., 26 (1999) 305.
13. D.J. Mitchell, G.I.T. Tiddy, J. Waring and T.J. McDonald . *Chem. Soc. Faraday Trans*., 79 (1983) 975.
14. P.N. Bartlett, P.R. Birikin, M.A. Ghanem, pde. Groot, and M. Sawicki. *J. Electrochem. Soc*.,148 (2001) C119.
15. L. Hongmei, S. Li, L.Yunfeng and Y. Yushan. *Langmuir*, 20 (2004) 10218.
16. I.S. El-Hallag. *Bull. Mater. Sci*., 32 (2009) 555.
17. L.Wang , J.Shi, J. Yu, and D. Yan, *Nanostruct. Mater*., 10 (1998) 1289.
18. M.A. Karakasside, A. Bourlions, D. Petridis, L. Coche-Guerente and P.J. Labbe. *Mater. Chem.*, 10 (2009) 403.
19. Y. Tan, S. Srinivasan and K.S. Choi. *J. Am. Chem. Soc.*, 127 (2005) 3596.
20. W.J. Zhou, D.D. Zhao, M-W. Xu, C.L. Xu and H-L. Li, *Electrochim. Acta*, 53 (2008) 7210.
21. M.H. Lee, S.G. Oh, K.D. Suh, D.G. Kim and D. Sohn.*Colloids Surf.*, 211 (2002) 49.
22. S. Cleverson, D. Rafaela, F. Luı´s, A.P. Christiana. *Arab J. Chem*., 13 (2020) 3448.
23. A.T. Chipeture, D. Apath, M. Moyo and M. Shumba. *J. Anal. Sci. Technol.*, 10 (2019) 22
24. E.R. Brown, and R.F. Large, (1971) Cyclic Voltammetry, A.C. Polarography and Related Techniques of Chemistry. In: E.R. Brown and R.F. Large, Eds., Physical Methods of Chemistry Electrochemical Methods, Vol. I, II-A, Wiley Interscience, New York, 423.

25. H. Gómez1, G. Riveros, D. Ramírez. *Int. J. Electrochem. Sci*., 12 (2017) 985.
26. Z. Zhang, H. Wu, Y. Gao , L. Huang , H. Pan , M. Du. *Int. J. Electrochem. Sc*i., 15 (2020) 2458.